RESTRICTED

CLASSIFICATION CANCELLED

NACA

RESEARCH MEMORANDUM

WIND—TUNNEL INVESTIGATION OF HORIZONTAL TAILS.

II — UNSWEPT AND 35° SWEPT—BACK PLAN FORMS OF

ASPECT RATIO 4.5

By Jules B. Dods, Jr.

Ames Aeronautical Laboratory
Moffett Field, Calif.

NATIONAL ADVISORY COMMITTEE
FOR AERONAUTICS
WASHINGTON
June 3, 1948

CLASSIFICATION CANCELLED

RESTRICTED

NATIONAL ADVISORY COMMITTEE FOR AERONAUTICS
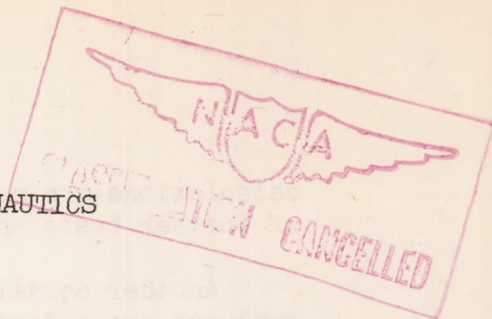
RESEARCH MEMORANDUM

WIND-TUNNEL INVESTIGATION OF HORIZONTAL TAILS.

II - UNSWEPT AND 35° SWEPT-BACK PLAN FORMS OF

ASPECT RATIO 4.5

By Jules B. Dods, Jr.

SUMMARY

The results of a wind-tunnel investigation of the low-speed aerodynamic characteristics of two semispan horizontal tails having unswept and 35° swept-back plan forms are presented. The two models had an aspect ratio of 4.5, taper ratio of 0.5, and an NACA 64A010 airfoil section. The data presented supplement previously reported results of tests of models having the same airfoil section, taper ratio, and sweepback, but with an aspect ratio of 3.0.

Test results are presented for the models with and without standard roughness applied to their leading edges and with sealed and unsealed radius-nose elevators.

The major effect of sweepback, as measured from the tests of the two models, was to reduce the rate of change of hinge-moment coefficient with elevator deflection and to reduce the elevator effectiveness. The difference between the rates of change of hinge-moment coefficient with angle of attack for the unswept and swept-back models was found to be negligible.

INTRODUCTION

A systematic investigation of the control-surface characteristics, particularly the hinge-moment parameters, of semispan horizontal tail surfaces has been undertaken by the NACA to provide experimental results for a comparison with those parameters computed by the lifting-surface theory. Reference 1 presented the experimental results obtained from wind-tunnel tests of models of aspect ratio 3, and the present report extends the experimental data to include an aspect ratio of 4.5. Comparisons with the theoretical

calculations are not presented herein, but will await the results of further tests and analysis.

Another equally important purpose of the investigation was to evaluate the effects of sweepback on the horizontal—tail parameters by a comparison of the results of tests of two models with the same aspect ratio, area, taper ratio, and airfoil section, differing mainly in the angle of sweepback.

COEFFICIENTS AND SYMBOLS

The coefficients and symbols as used throughout the report are defined as follows:

C_L lift coefficient (L/qS)

C_{h_e} elevator hinge—moment coefficient $(H/qS_e\bar{c}_e)$ (See appendix.)

C_m pitching—moment coefficient $[M/qS(M.A.C.)]$

$\Delta p/q$ pressure coefficient across elevator—nose seal (pressure below seal minus pressure above seal divided by the dynamic pressure)

A aspect ratio $(2b^2/S)$

α corrected angle of attack, degrees

b span of the semispan model measured perpendicular to the plane of symmetry, feet

b_e' span of the elevator of the semispan model measured along the hinge line, feet

c chord of the semispan model measured parallel to the plane of symmetry, feet

c_e' chord of the elevator aft of the hinge line measured perpendicular to the hinge line, feet

$\bar{c}_e$ root—mean—square elevator chord aft of the hinge line measured parallel to the plane of symmetry, feet

$\bar{c}_e'$ root—mean—square elevator chord aft of the hinge line measured perpendicular to the hinge line, feet

δ_e elevator deflection (positive when trailing edge of elevator is down) measured in a plane normal to the hinge line, degrees
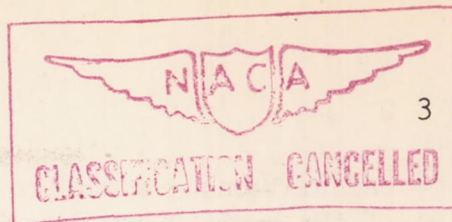
H	hinge moment, foot-pounds
L	lift, pounds
M	pitching moment about a lateral axis through the 0.25 M.A.C. point, foot-pounds
M_A	first moment of the elevator area aft of the hinge line about the hinge line, cubic feet
M.A.C.	mean aerodynamic chord, feet
q	free-stream dynamic pressure $(\frac{1}{2}\rho V^2)$, pounds per square foot
R	Reynolds number $\left[\dfrac{\rho V(\text{M.A.C.})}{\mu}\right]$
ρ	density of air, slugs per cubic foot
μ	absolute viscosity, slugs per foot-second
V	velocity of air, feet per second
S	area of semispan horizontal tail, square feet
S_e	area of semispan elevator aft of hinge line, square feet

In addition, the following symbols are used:

$$C_{L_\alpha} = \left(\frac{\partial C_L}{\partial \alpha}\right)_{\delta_e = 0} \quad \text{(measured through } \alpha = 0\text{)}$$

$$C_{L_{\delta_e}} = \left(\frac{\partial C_L}{\partial \delta_e}\right)_{\alpha = 0} \quad \text{(measured through } \delta_e = 0\text{)}$$

$$C_{h_\alpha} = \left(\frac{\partial C_{h_e}}{\partial \alpha}\right)_{\delta_e = 0} \quad \text{(measured through } \alpha = 0\text{)}$$

$$C_{h_{\delta_e}} = \left(\frac{\partial C_{h_e}}{\partial \delta_e}\right)_{\alpha = 0} \quad \text{(measured through } \delta_e = 0\text{)}$$

$$\alpha_{\delta_e} = -\frac{C_{L_{\delta_e}}}{C_{L_\alpha}} \qquad \text{elevator-effectiveness parameter}$$

MODELS

The models tested in this investigation had an aspect ratio of 4.5 and a taper ratio (ratio of tip chord to root chord) of 0.5. The 0.25-chord lines were swept back 7.6° for the unswept model and 35° for the swept-back model, as shown in figure 1.

The airfoil sections were the same as for the models of reference 1. The slight discrepancies between the model coordinates and the true NACA 64A010 coordinates (table I) are not considered important. The airfoil sections were perpendicular to the 0.70-chord line (elevator hinge line) for the unswept plan form and perpendicular to the 0.25-chord line for the swept-back plan form.

Both models were equipped with sealed radius-nose elevators. For the unswept model the elevator chord aft of the hinge line was 0.30 of the tail chord perpendicular to the 0.70-chord line. The elevator chord of the swept-back model was 0.30 of the tail chord perpendicular to the 0.25-chord line. (See fig. 1(b).) Because the elevator-chord ratios were held constant in the manner explained above, the ratios of elevator area to total surface area were different (0.300 for the unswept model and 0.271 for the swept-back model).

The gaps between the elevators and the shrouds and the gaps between the elevator noses and the balance plates (seal gap) are shown in figure 1. Pressure orifices were located in the balance chambers enclosed by the shrouds both above and below the seal at four spanwise stations. In addition to the seal across the elevator-nose gap, the ends of the balance chamber were sealed at the root section and at the outboard hinge bracket. The pressure orifices at 91 percent span were outboard of the elevator hinge bracket.

The tip shapes were formed by rotating the tip airfoil section parallel to the undisturbed air stream about a line inboard of the tip, a distance equal to the maximum tip ordinate.

Photographs showing the models mounted in the wind tunnel are given in figures 2 and 3.

TESTS

The models were mounted on a turntable flush with the floor of one of the Ames 7— by 10—foot wind tunnels. (See figs. 2 and 3.) The tests were conducted with a dynamic pressure of 57 pounds per square foot, corresponding to a Reynolds number of 3.0×10^6. For those tests with leading—edge roughness, standard roughness was applied in the manner described in reference 2.

Model lift and pitching moment were measured by the wind—tunnel balance system. Elevator hinge moments were measured by a resistance—type torsional strain gage. Pressures above and below the elevator—nose seal in the balance chamber were measured by a manometer connected to the orifices in the balance chamber.

All coefficients and the angle of attack have been corrected for the effects of the tunnel walls by methods similar to those of reference 3. The corrections listed below were added to the data for both the unswept and the swept—back models:

$$\Delta\alpha_1 = 0.950 \; C_{L_u}$$

$$\Delta\alpha_2 = 0.108 \; C_{L_u} \; (\delta_e = 0)$$

$$\Delta C_m = 0.00307 \; C_{L_u}$$

$$\Delta C_{h_e} = 0.00424 \; C_{L_u}$$

$$C_L = 0.994 \; C_{L_u}$$

where

$\Delta\alpha_1$ jet—boundary correction to angle of attack

$\Delta\alpha_2$ streamline—curvature correction to angle of attack

ΔC_m correction to pitching—moment coefficient

ΔC_{h_e} correction to hinge—moment coefficient

C_{L_u} uncorrected lift coefficient

RESULTS AND DISCUSSION

The results of tests of the unswept tail are presented in figures 4 to 8 and those for the swept-back tail are presented in figures 9 to 13. The variations of lift, hinge-moment, and pitching-moment coefficients with angle of attack are given in figures 4 and 9. Hinge-moment coefficients are also shown as a function of the elevator angle for various angles of attack in figures 5 and 10. In addition, the variation of the pressure ccefficient across the elevator-nose seal with angle of attack is presented in figures 6 and 11. The effects of standard leading-edge roughness and removal of the elevator seal on the lift and hinge-moment coefficients are shown in figures 7 and 8 for the unswept model and in figures 12 and 13 for the swept-back model. A summary of the parameters measured is given in table II.

Effectiveness and Hinge-Moment Parameters

The lift effectiveness and the hinge-moment parameters are listed in table II for the two tails. As shown in the table, C_{h_α} changed from -0.0020 for the unswept model to -0.0021 for the swept-back model; the change in $C_{h_{\delta_e}}$ was from -0.0095 to -0.0069, and the elevator-effectiveness parameter α_{δ_e} was changed from -0.68 to -0.52. The value of $C_{L_{\delta_e}}$ was reduced from 0.045 to 0.032, and C_{L_α} was reduced from 0.066 to 0.061. Although the major part of the change in parameters can be attributed to sweepback, the possibility of effects due to the difference in the ratio of elevator area to total surface area between the two models should be noted.

Static Longitudinal Stability

The pitching moments about the one-quarter M.A.C. point indicate a stabilizing effect of sweepback. The unswept model was statically unstable $[(dC_m/d\alpha)_{\delta_e} = 0.0014$ measured through zero angle of attack], while the swept-back model was neutrally stable. A negative deflection of the elevators reduced the stability of both models as shown in figures 4(c) and 9(c).

Reference 4 would predict that, at the stall, the static longitudinal stability of the unswept model would increase markedly and that the stability of the swept-back model would be marginal. The

experimental results of figures 4(c) and 9(c) agree with this pre-
diction.

Effect of Standard Roughness

The effects of standard leading-edge roughness (elevator sealed)
upon the lift and hinge-moment coefficients are shown in figure 7 for
the unswept model and in figure 12 for the swept-back model.

Standard roughness on the unswept model increased the maximum
lift coefficient by 0.04 with the elevator undeflected, and by
0.10 with the elevator deflected either down 4° or up 15°. These
increases were obtained primarily because of a delay in the angle
of stall. The improvement in the lift characteristics by roughness
also resulted in less severe changes in the hinge-moment coeffi-
cients near the stall. The value of C_{h_α} of -0.0020 for the smooth
unswept model was changed to -0.0018 by the addition of standard
roughness, and $C_{h_{\delta_e}}$ was changed from -0.0095 to -0.0080.

Standard roughness on the swept-back tail had little effect
on the maximum lift coefficients for any elevator deflection or on
the hinge-moment coefficients near the stall. The value of C_{h_α} of
-0.0021 for the smooth swept-back tail was changed to -0.0024 by
roughness, and $C_{h_{\delta_e}}$ was changed from -0.0069 to -0.0064. These
effects of roughness on the characteristics of the models having
an aspect ratio of 4.5 were considerably greater than those measured
for the unswept and the swept-back models of aspect ratio 3
(reference 1).

As shown in figure 4(a), a different type of stall was measured
for the unswept model at positive and negative angles of attack. A
similar result was found for the unswept model of reference 1. Tuft
studies have indicated that this difference does exist. Measurements
have shown that the twist of the models was negligible and that the
contours of the upper and lower surfaces were not appreciably
different. Thus, the reason for the unsymmetrical stall is not
understood.

Effect of Removing Elevator-Nose Seal

The greatest effect of removing the elevator-nose seal (models
in smooth condition) was to reduce the lift-effectiveness parameter
$C_{L_{\delta_e}}$. As shown in table II, $C_{L_{\delta_e}}$ was reduced from 0.045 to 0.041

(9 percent) for the unswept tail, and it was reduced from 0.032 to
0.030 (6 percent) for the swept—back tail. The hinge—moment parame—
ters were relatively unaffected for either tail. However, for large
elevator deflections, an appreciable change in the hinge—moment
coefficients was measured, as shown in figures 8(b) and 13(b).

CONCLUSIONS

The results of tests conducted to determine the low—speed aero—
dynamic characteristics of horizontal tails of aspect ratio 4.5
having unswept and swept—back plan forms indicate that:

1. The value of $C_{h_{\delta_e}}$ was changed from −0.0095 for the
unswept tail to −0.0069 for the 35° swept—back tail. The change in
C_{h_α} was negligible.

2. The elevator—effectiveness parameter α_{δ_e} was changed from
−0.68 for the unswept model to −0.52 for the swept—back model.

3. The effect of standard leading—edge roughness was greater
for the unswept model than for the swept—back model. The maximum
lift coefficient of the unswept tail was increased from 0.87 to 0.91
with an elevator deflection of 0°, and the changes of hinge—moment
coefficient were less severe near the stall. Practically no effect
of roughness was observed for the swept—back tail.

4. Removal of the elevator—nose seal had the greatest effect
upon the elevator effectiveness of the unswept tail. The hinge—
moment parameters were relatively unaffected for both tails.

Ames Aeronautical Laboratory,
    National Advisory Committee for Aeronautics,
        Moffett Field, Calif.

REFERENCES

1. Dods, Jules B., Jr.: Wind—Tunnel Investigation of Horizontal
        Tails. I − Unswept and 35° Swept—Back Plan Forms of Aspect
        Ratio 3. NACA RM No. A7K24, 1947.

2. Abbott, Ira H., von Doenhoff, Albert E., and Stivers, Louis S., Jr.:
        Summary of Airfoil Data. NACA ACR No. L5C05, 1945.

3. Swanson, Robert S., and Toll, Thomas A.: Jet—Boundary Correc-
     tions for Reflection—Plane Models in Rectangular Wind Tunnels.
     NACA ARR No. 3E22, 1943.

4. Shortal, Joseph A., and Maggin, Bernard: Effect of Sweepback
     and Aspect Ratio on Longitudinal Stability Characteristics
     of Wings at Low Speeds. NACA TN No. 1093, 1946.

APPENDIX

Conversion Factors for Hinge—Moment Coefficients

Because several methods are in use for the computation of hinge—
moment coefficients, particularly for swept—back lifting surfaces,
conversion factors for the various methods are presented. To obtain
the hinge—moment coefficients for one of the listed methods, multiply
the value of the hinge—moment coefficients of this report by the
corresponding conversion factor in the following table:

Equations for hinge—moment coefficients	Unswept model		Swept—back model	
	$\dfrac{H}{qC_{h_e}}$ (ft^3)	Conversion factor	$\dfrac{H}{qC_{h_e}}$ (ft^3)	Conversion factor
$C_{h_e} = \dfrac{H}{qS_e\overline{c}_e}$	1.956	1.000	1.594	1.000
$C_{h_e} = \dfrac{H}{qb\overline{c}_e{}^2}$	1.994	.981	1.624	.982
$C_{h_e} = \dfrac{H}{qb_e{}'c_e{}'^2}$	1.994	.981	1.410	1.130
$C_{h_e} = \dfrac{H}{2qMA}$	1.994	.981	1.410	1.130

TABLE I.— COORDINATES FOR THE NACA 64A010
AIRFOIL AND THE MODELS TESTED

[All Dimensions in Percent of Wing Chord]

Upper and Lower Surfaces		
Station	NACA 64A010 ordinate	Model ordinate
0	0	0
.50	.804	.819
.75	.969	.987
1.25	1.225	1.247
2.50	1.688	1.696
5.00	2.327	2.333
7.50	2.805	2.780
10.00	3.199	3.202
15.00	3.813	3.816
20.00	4.272	4.280
25.00	4.606	4.610
30.00	4.837	4.842
35.00	4.968	4.950
40.00	4.995	4.975
45.00	4.894	4.889
50.00	4.684	4.672
55.00	4.388	4.373
60.00	4.021	4.011
65.00	3.597	3.594
70.00	3.127	3.131
75.00	2.623	2.637
80.00	2.103	2.120
85.00	1.582	1.595
90.00	1.062	1.071
95.00	.541	.553
100.00	.021	0
L.E. radius 0.687[a] T.E. radius 0.023[a]		

[a]Same for NACA 64A010 airfoil and
model ordinates.

NACA

TABLE II.— A SUMMARY OF THE LIFT AND HINGE—MOMENT
PARAMETERS OF THE UNSWEPT AND 35° SWEPT—BACK
MODELS OF ASPECT RATIO 4.5

Parameter	Models in normal condition	Models with standard leading-edge roughness	Elevator-nose seal removed
Unswept			
C_{h_α}	−0.0020	−0.0018	−0.0020
$C_{h_{\delta_e}}$	−.0095	−.0080	−.0096
C_{L_α}	.066	.066	.066
$C_{L_{\delta_e}}$	.045	.042	.041
α_{δ_e}	−.68	−.64	−.62
Swept—back			
C_{h_α}	−0.0021	−0.0024	−0.0021
$C_{h_{\delta_e}}$	−.0069	−.0064	−.0067
C_{L_α}	.061	.062	.059
$C_{L_{\delta_e}}$	.032	.032	.030
α_{δ_e}	−.52	−.52	−.51

NACA

Figure I.- Plan forms of the horizontal tail models of aspect ratio 4.5.

(a) Three-quarter front view.

(b) Side view.

Figure 2.— The unswept tail mounted in the 7— by 10—foot wind tunnel.
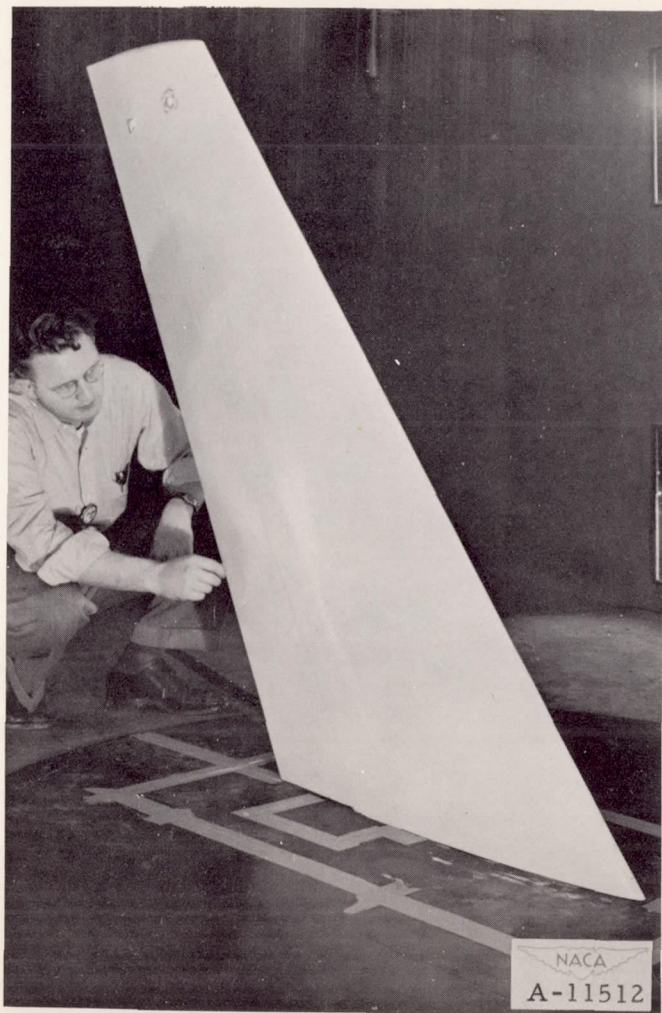
(a) Three-quarter front view.

(b) Three-quarter rear view.

Figure 3.— The 35° swept—back tail mounted in the 7— by 10—foot wind tunnel.
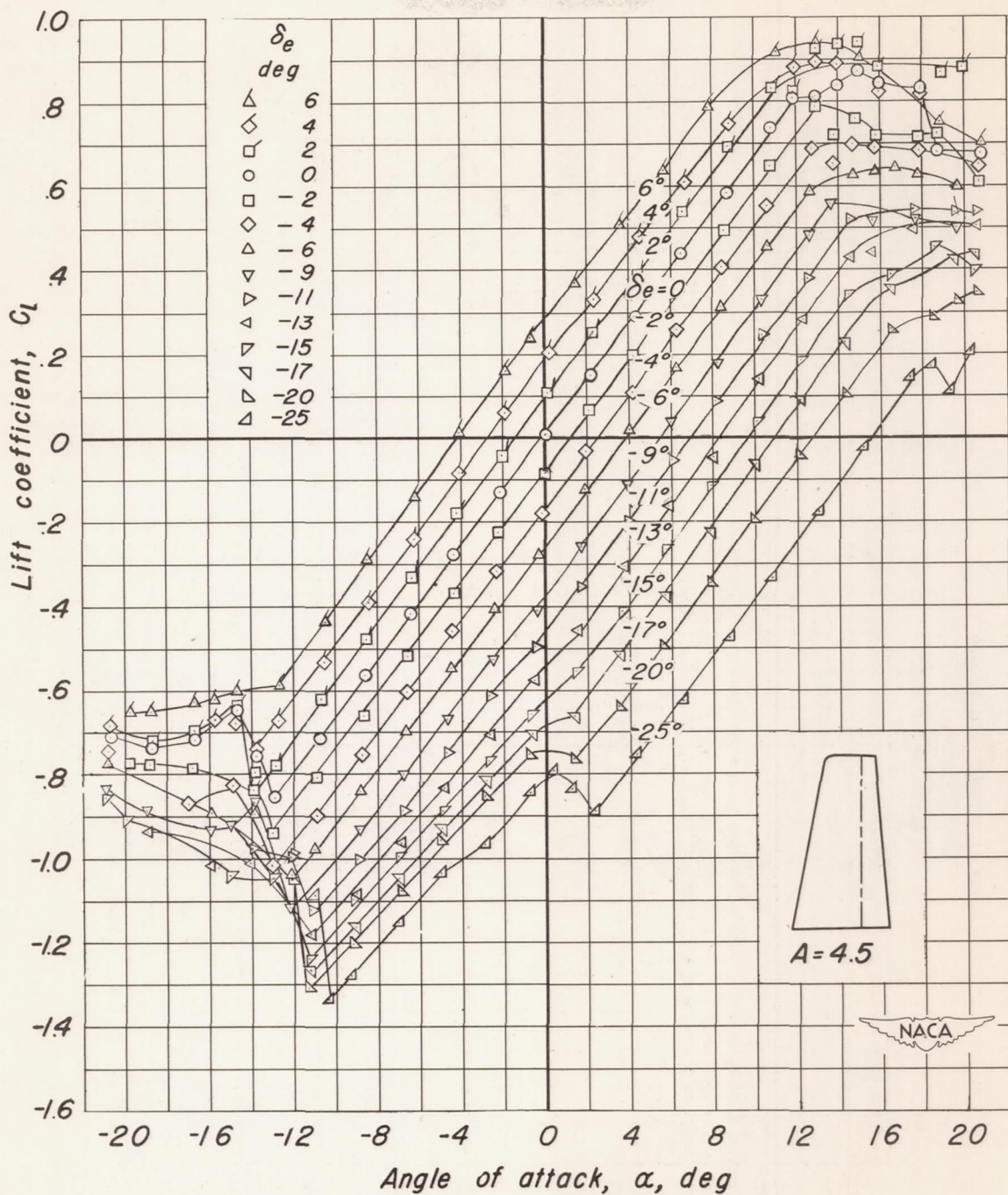
(a) Lift coefficient

Figure 4.- Lift, hinge-moment, and pitching-moment coefficients
of the unswept tail. Aspect ratio 4.5; R, 3.0 x 10^6.
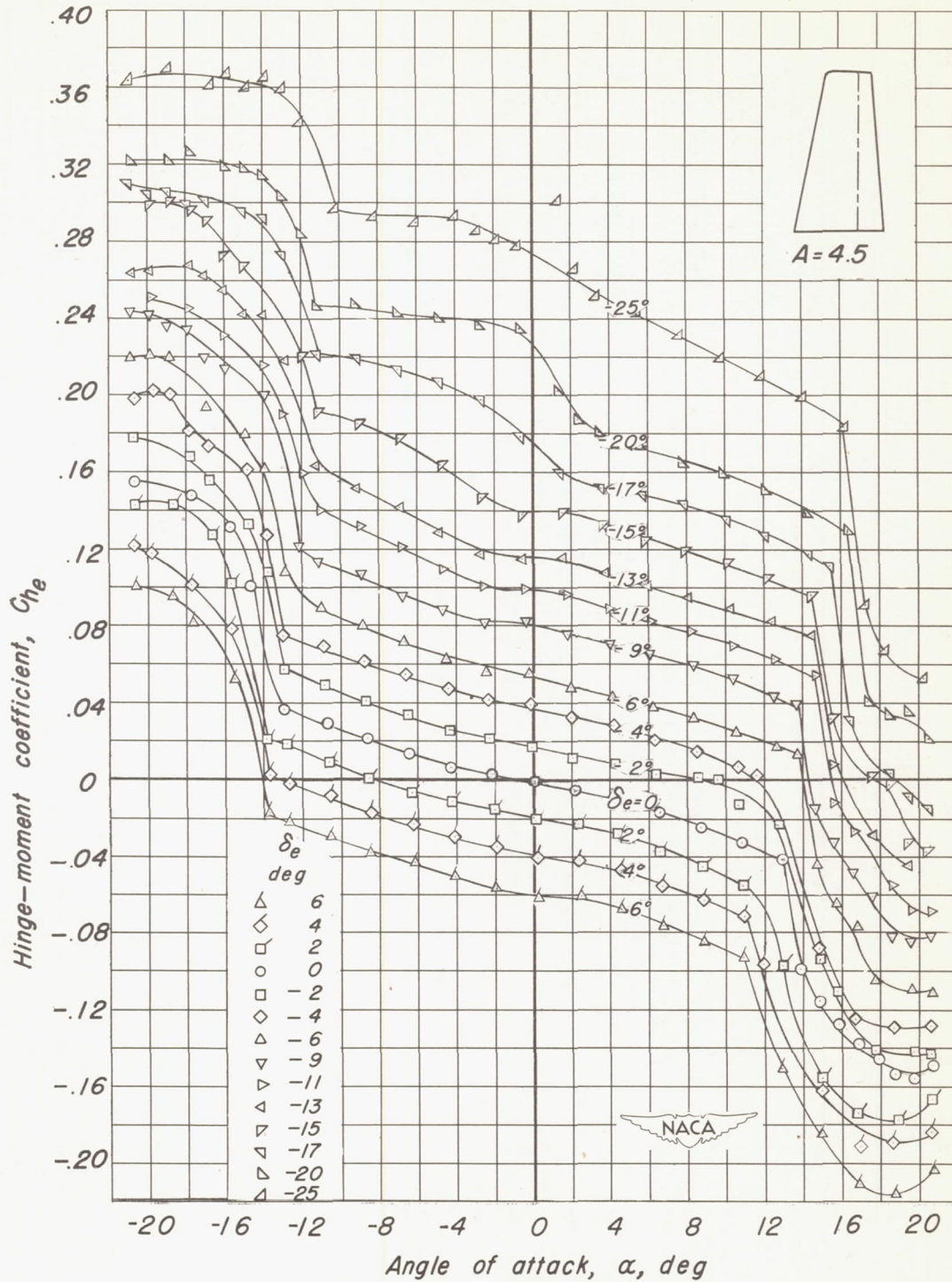
(b) Hinge-moment coefficient

Figure. 4 — continued.
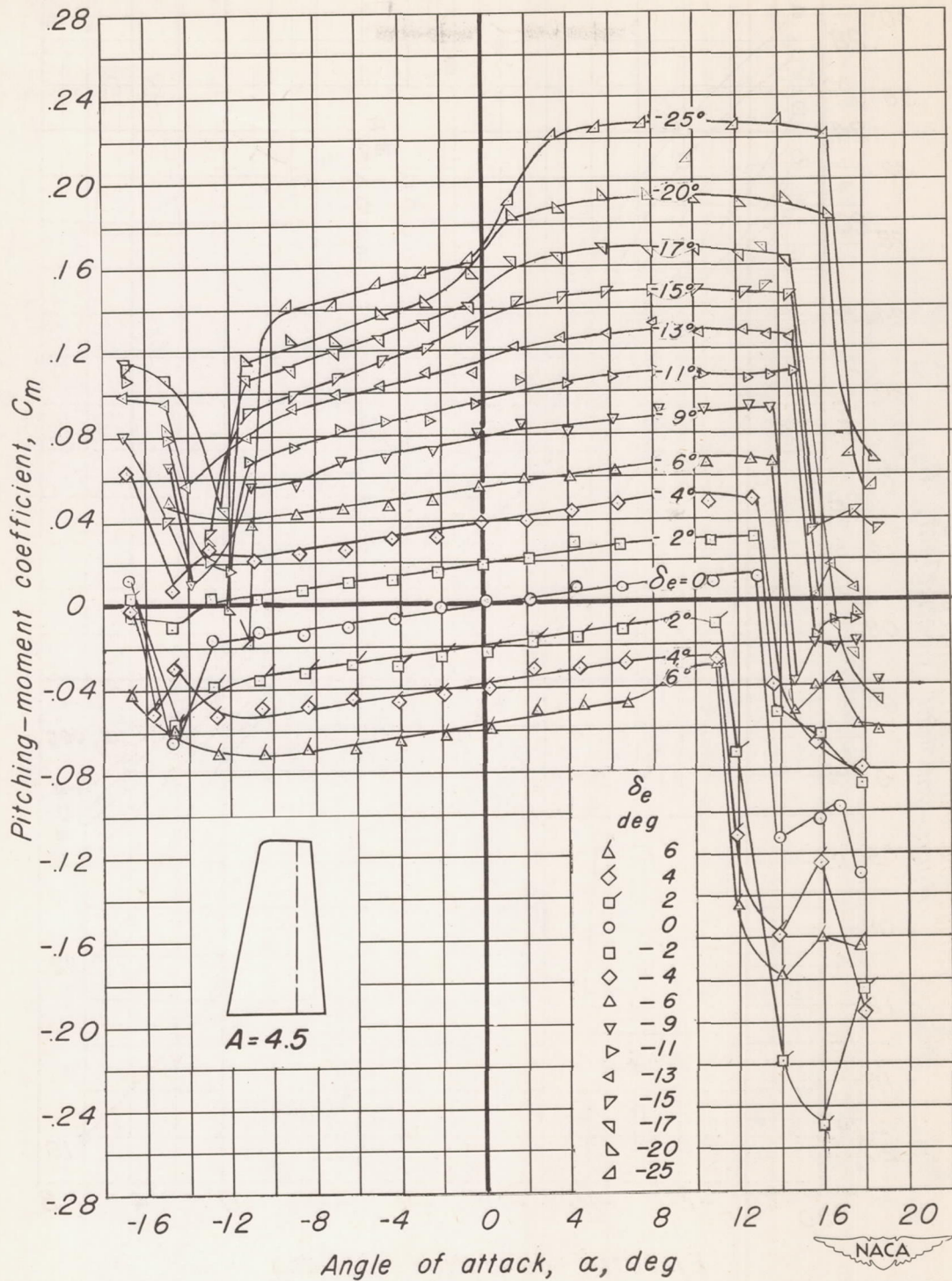
(c) Pitching—moment coefficient

Figure. 4 —concluded.
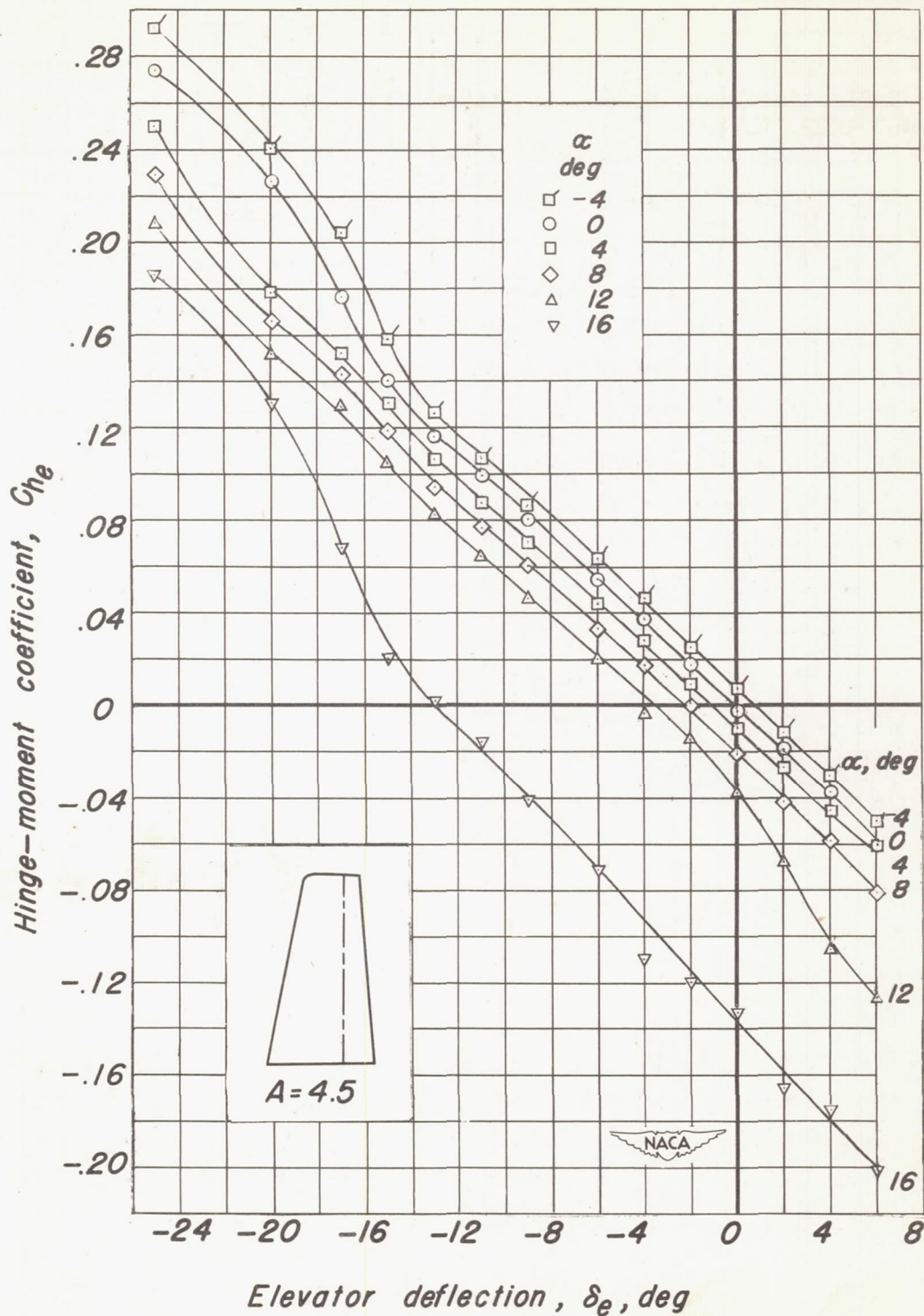
Figure 5.- Variation of hinge-moment coefficient with elevator deflection for various angles of attack of the unswept tail. Aspect ratio, 4.5; R, 3.0 x 10^6.
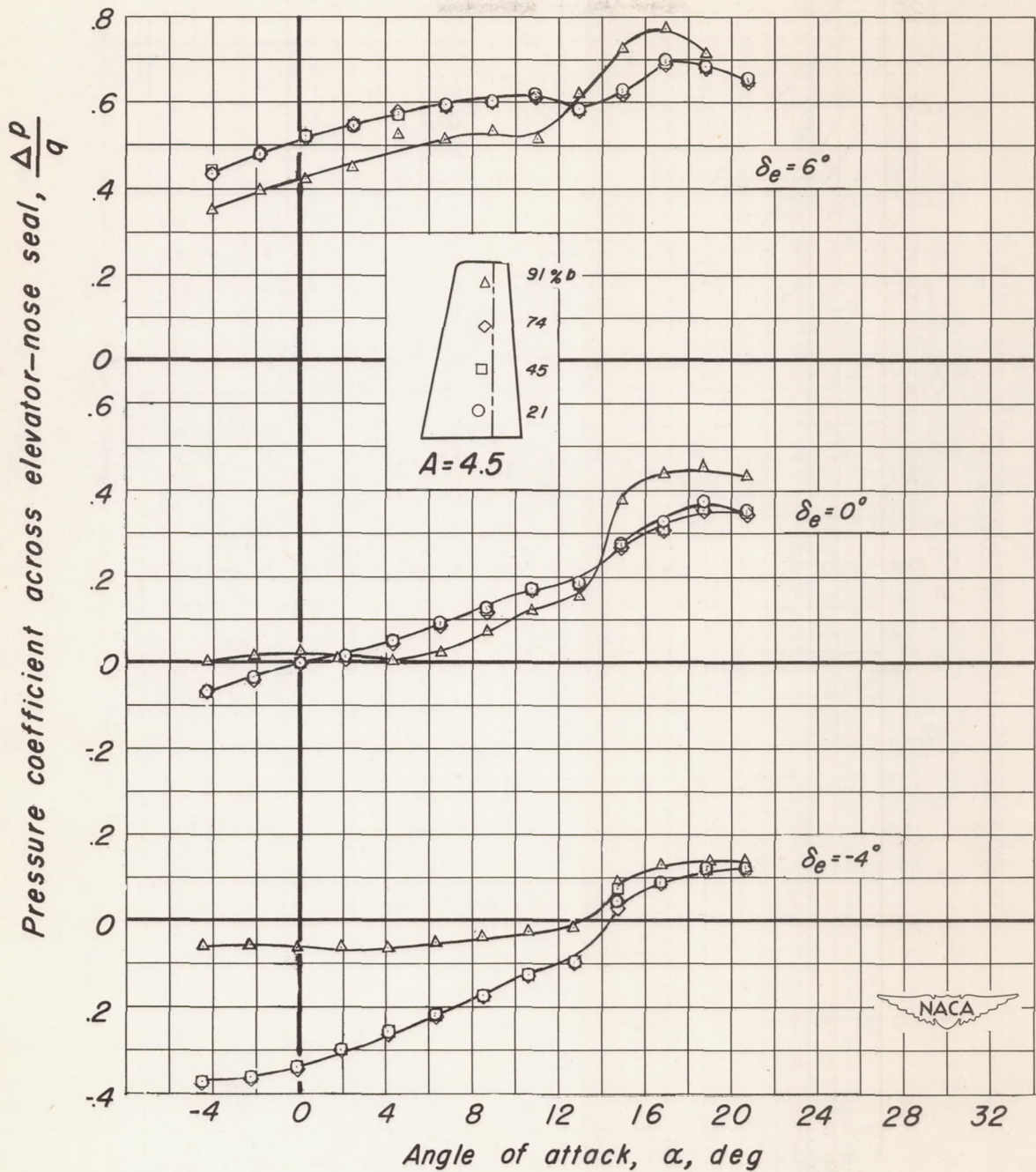
(a) δ_e = 6°, 0°, -4°.

Figure 6.- Variation of pressure coefficient across elevator-nose seal with angle of attack of the unswept tail. Aspect ratio, 4.5; R, 3.0 x 10⁶.
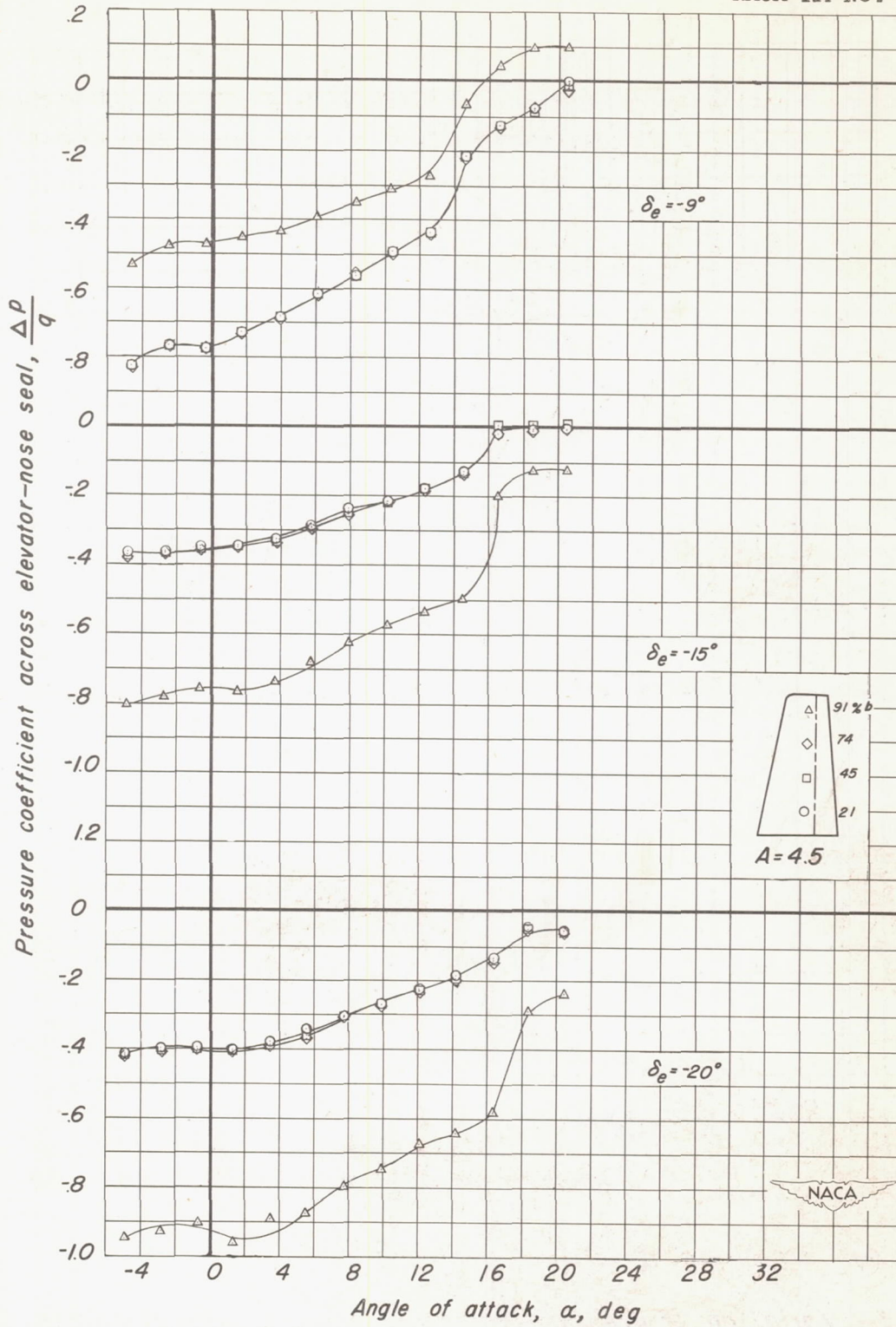
(b) δ_e = -9°, -15°, -20°

Figure. 6   —concluded.
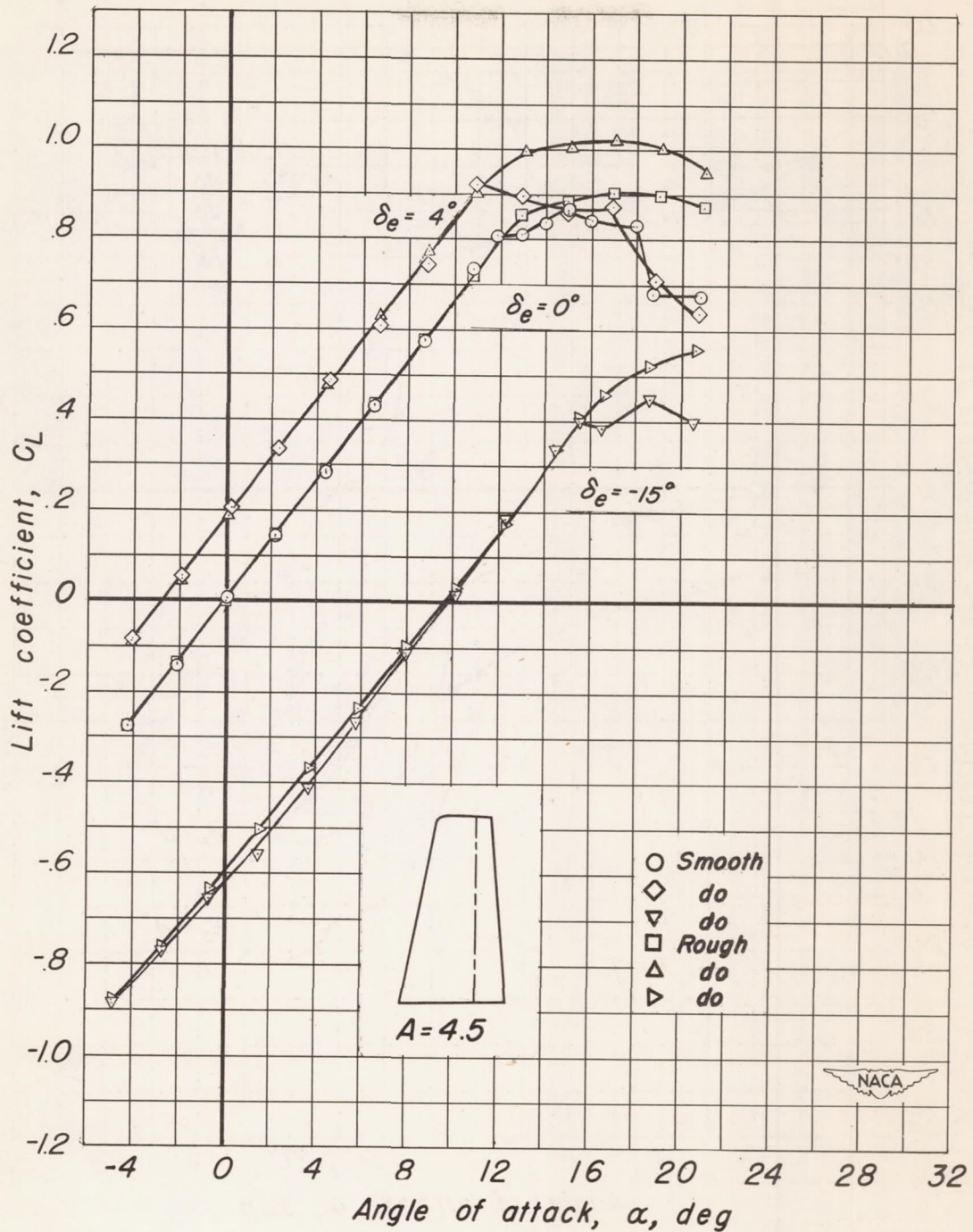
(a) Lift coefficient

Figure 7.— Comparison of the lift and hinge-moment coefficients of the smooth and rough unswept tail. Aspect ratio, 4.5; R, 3.0 x 10^6.
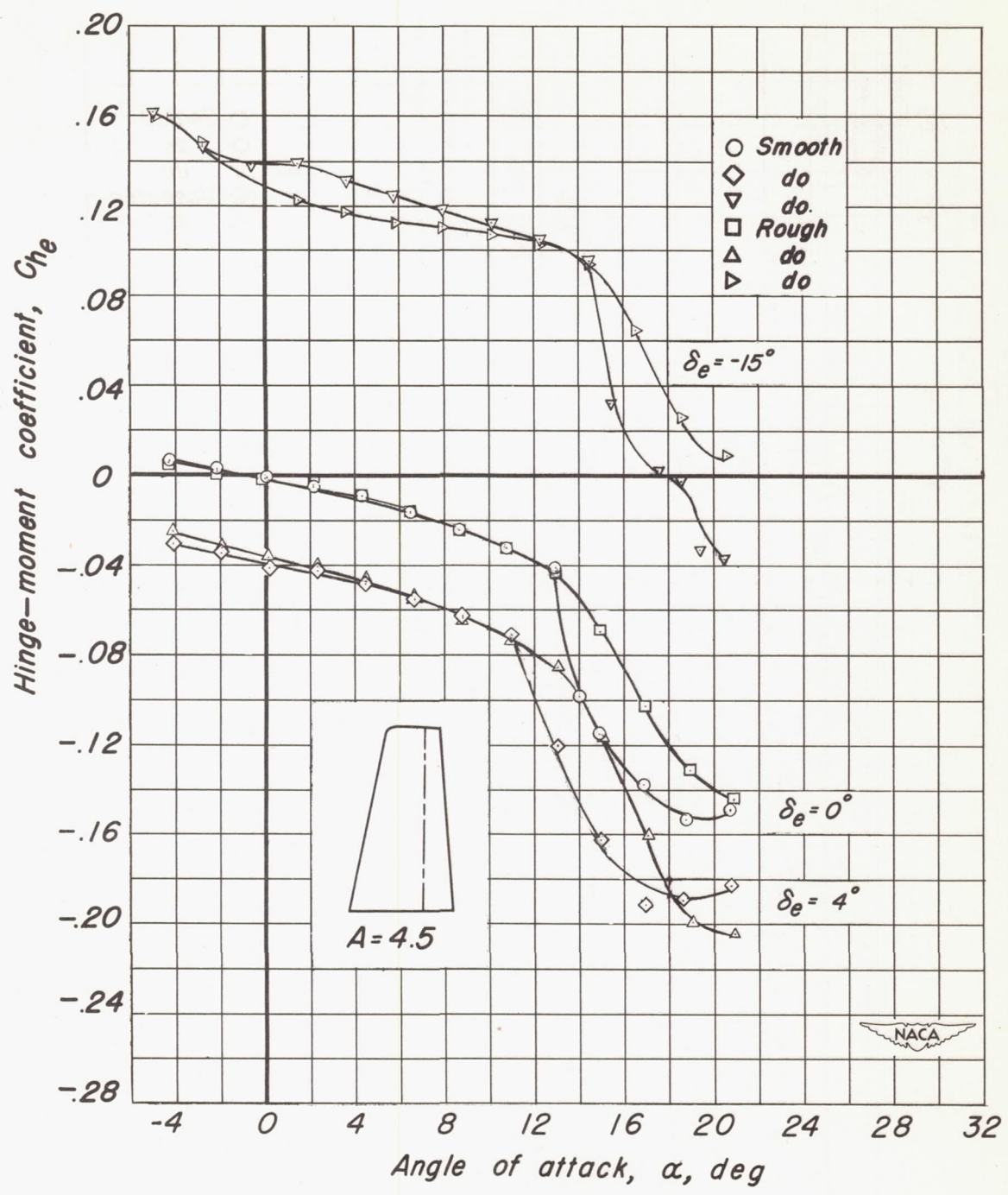
(b) Hinge-moment coefficient

Figure. 7 —concluded.
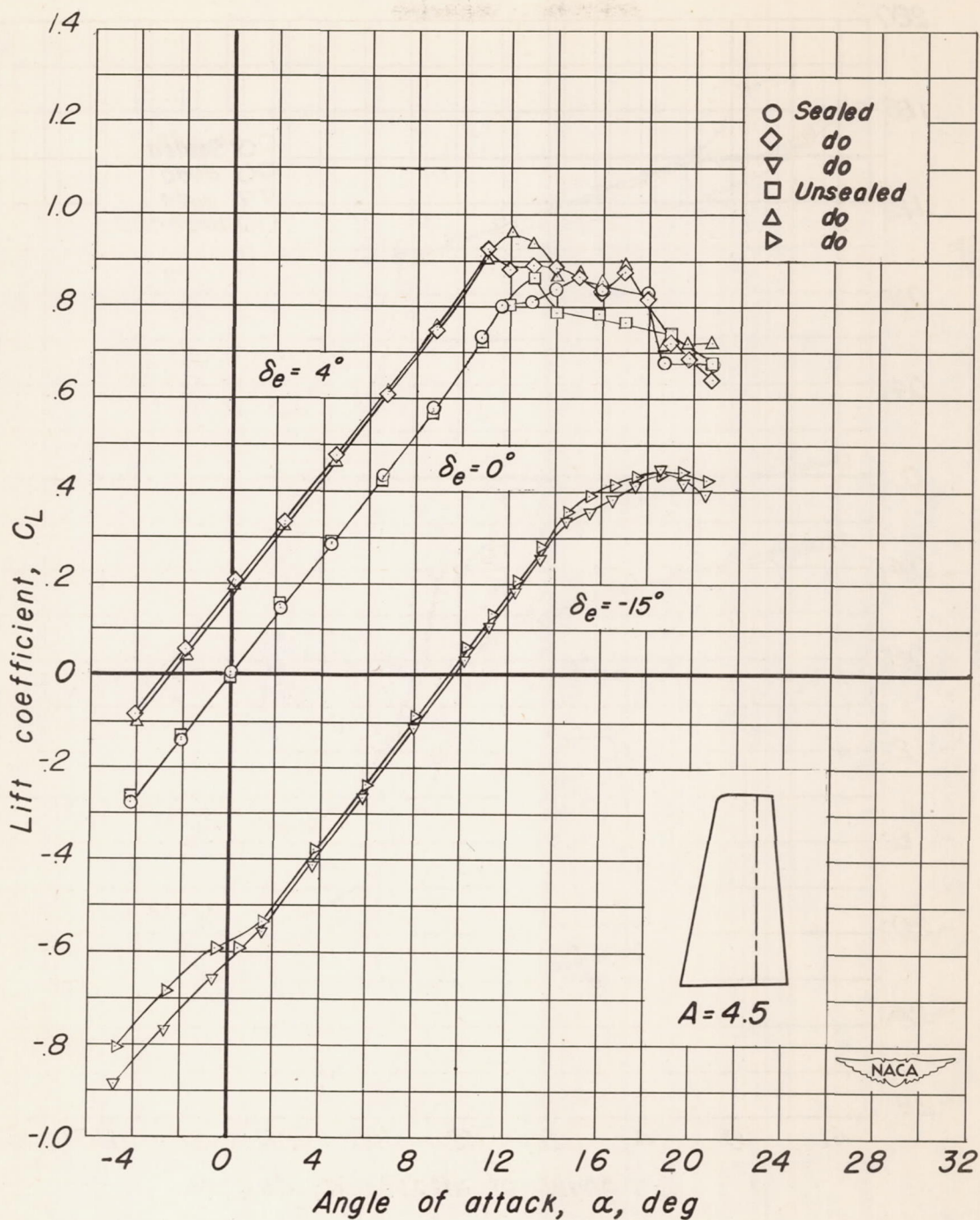
(a) Lift coefficient.

Figure 8.— Comparison of the lift and hinge-moment
coefficients with and without elevator seal on the
unswept tail. Aspect ratio, 4.5; R, 3.0 x 10^6.
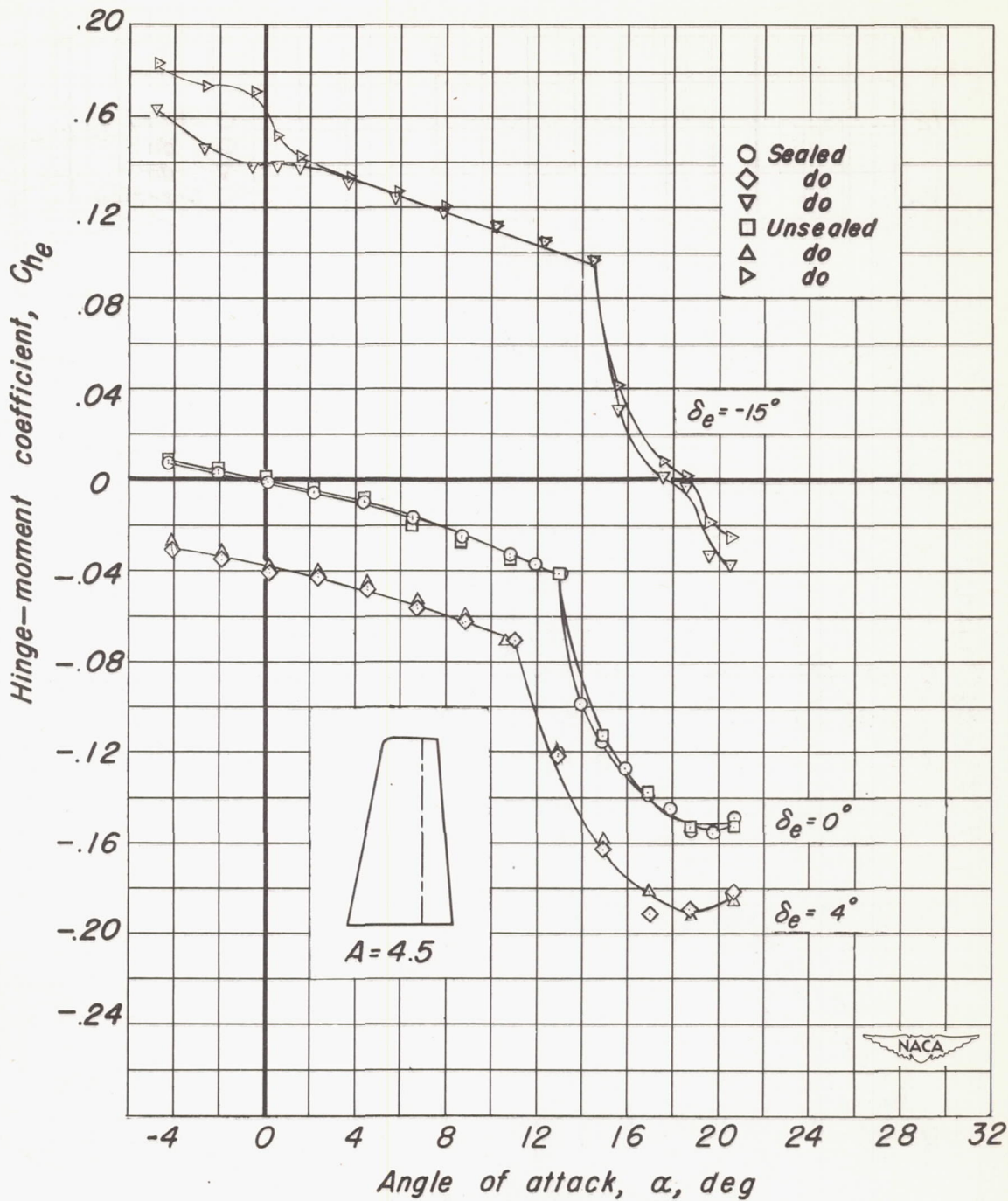
(b) Hinge-moment coefficient.

Figure. 8 —concluded.
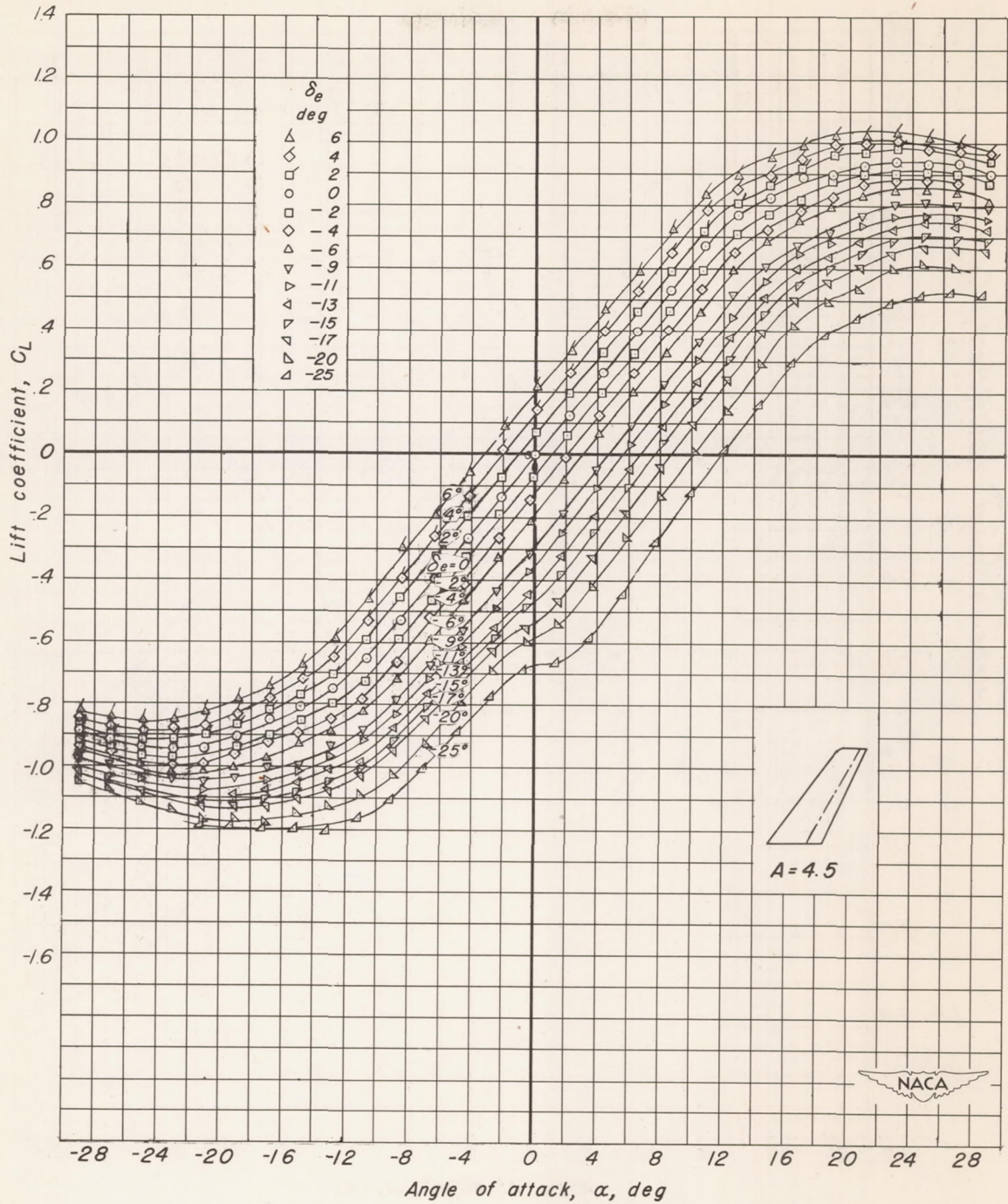
(a) Lift coefficient.

Figure 9.– Lift, hinge-moment, and pitching-moment coefficients of the 35° swept-back tail. Aspect ratio, 4.5; R, 3.0 x 10^6.
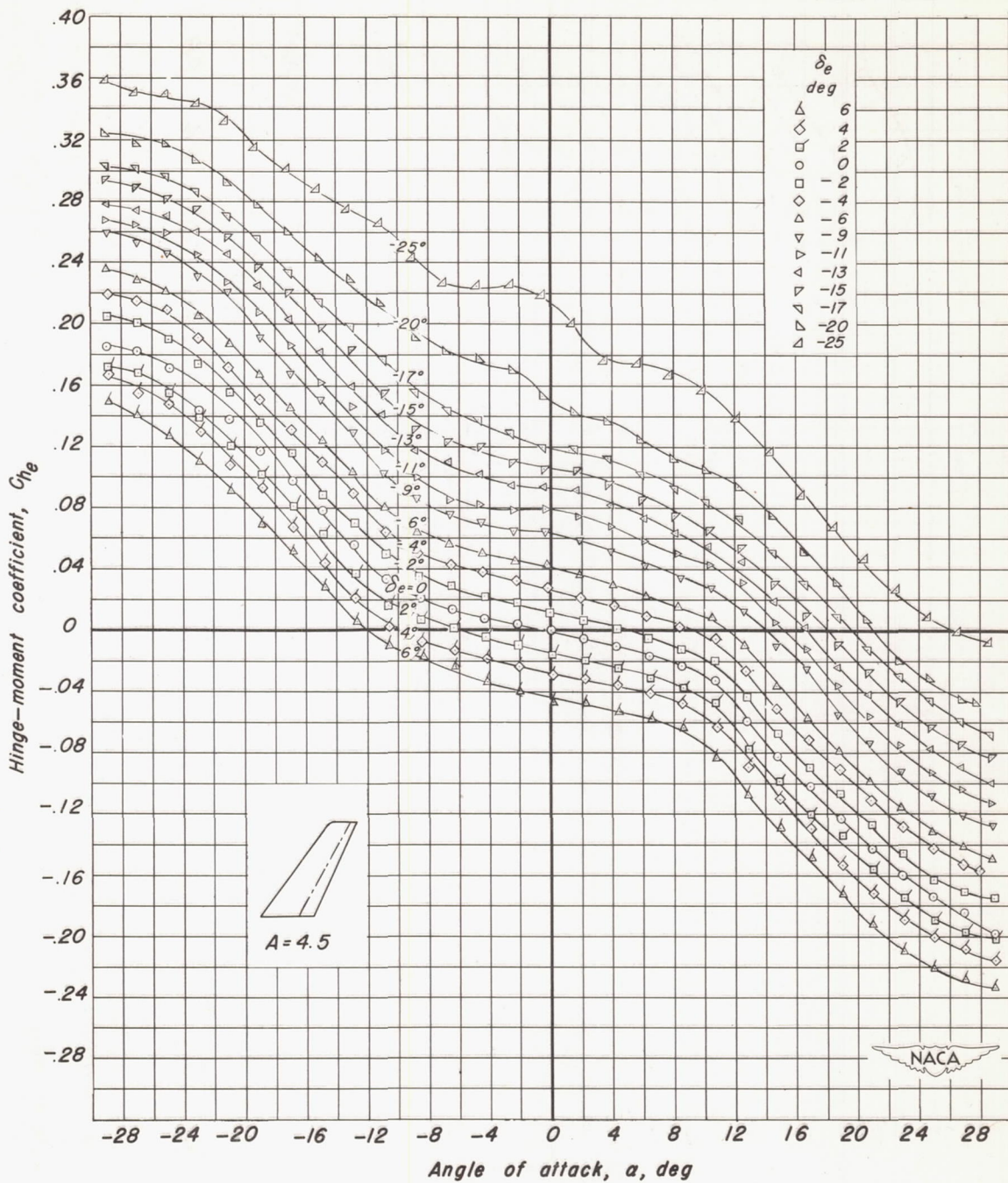
(b) Hinge-moment coefficient

Figure. 9　— continued.
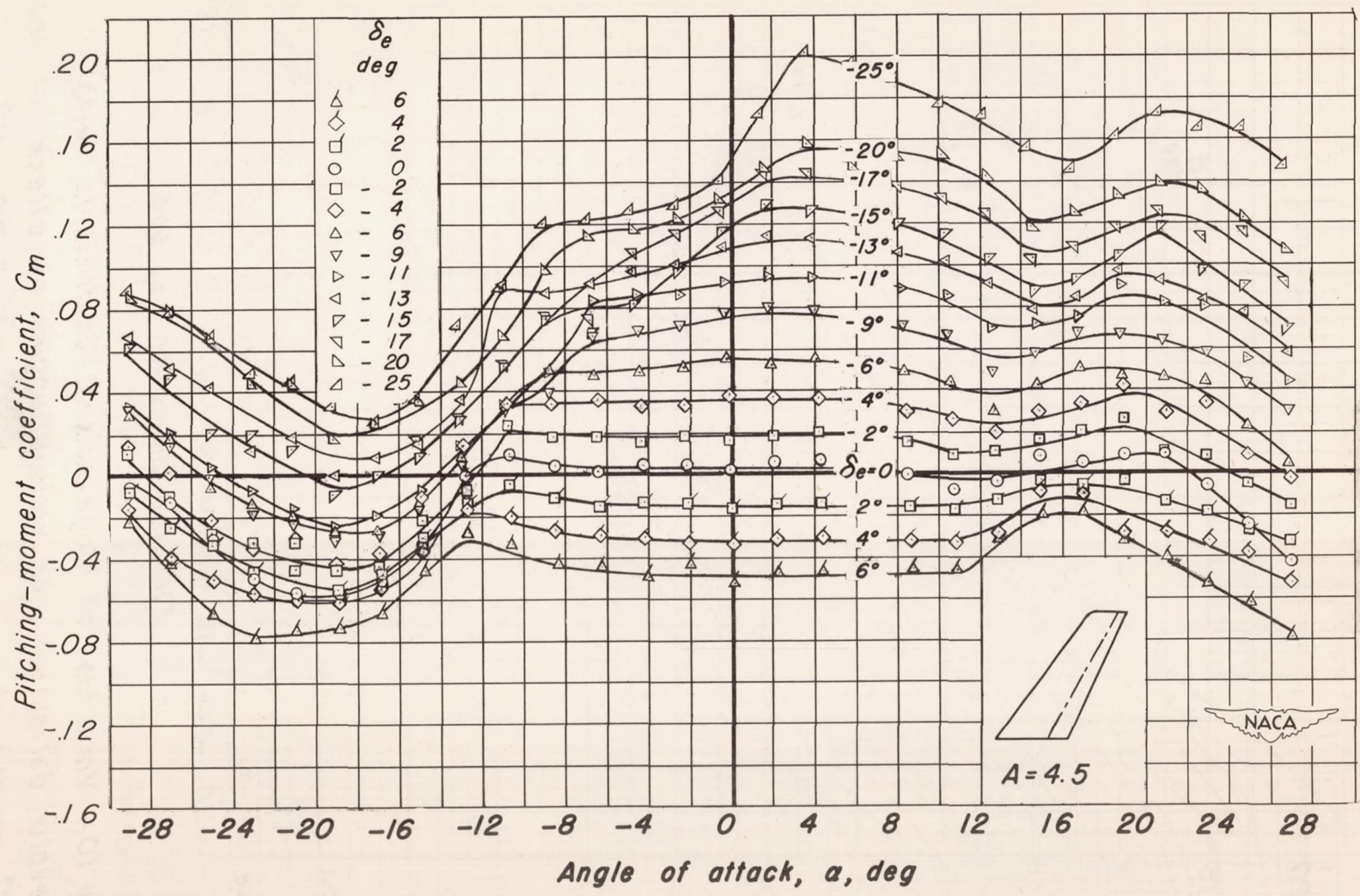
(c) Pitching–moment coefficient.

Figure. 9 —concluded.
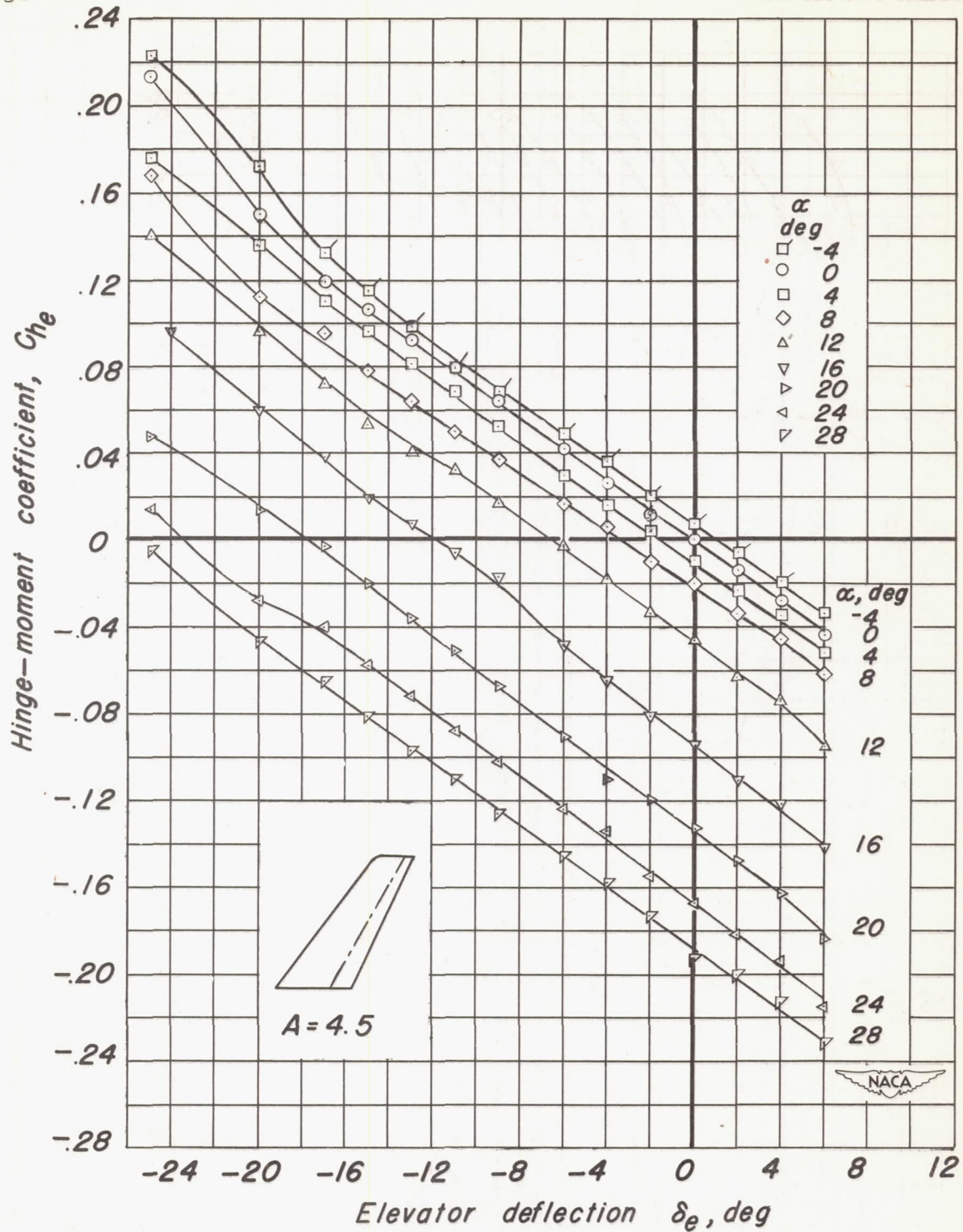
Figure 10.— Variation of hinge-moment coefficients with elevator deflection for various angles of attack of the 35° swept-back tail. Aspect ratio, 4.5; R, 3.0 x 10⁶.
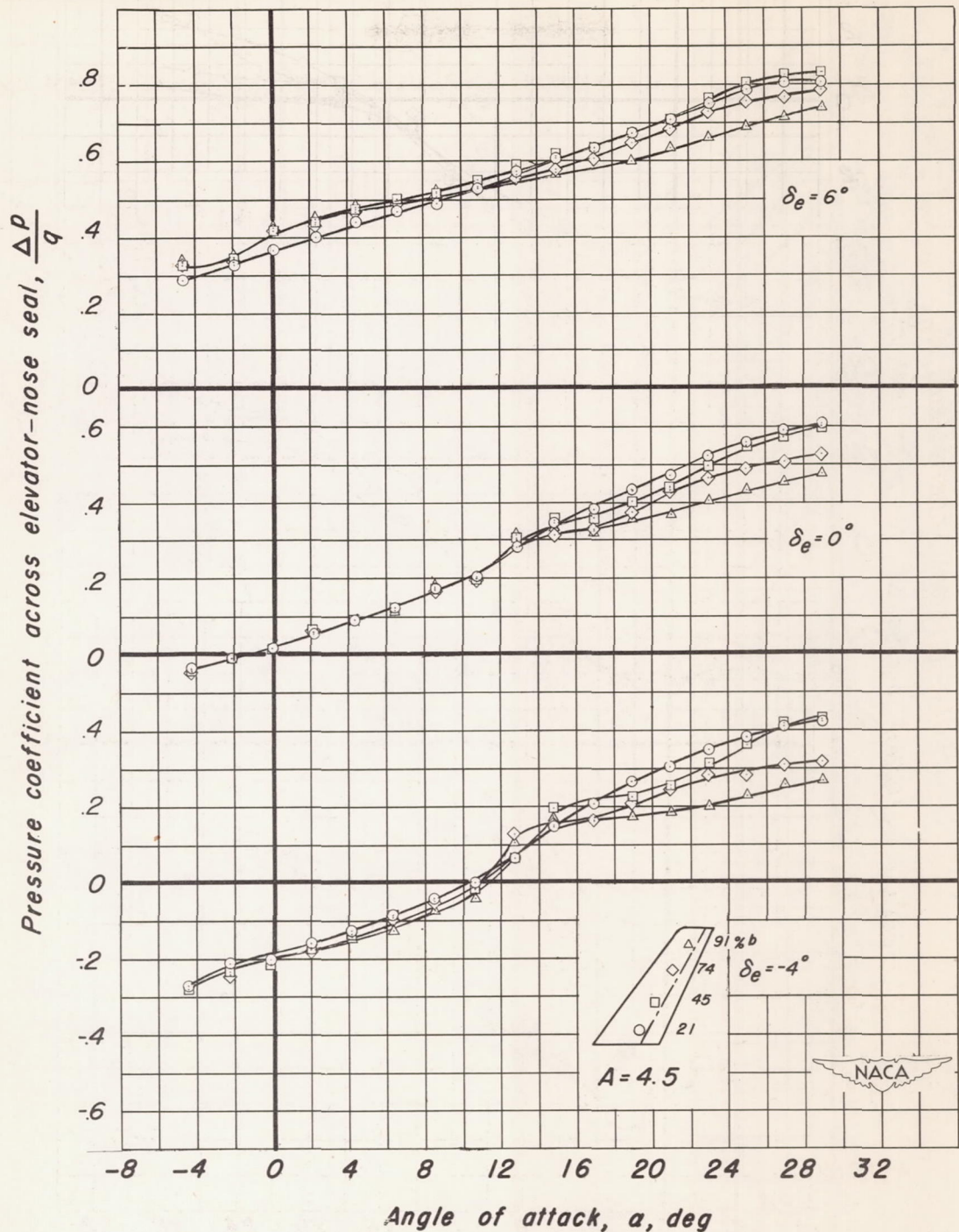
(a) δ_e = 6°, 0°, -4°.

Figure 11.— Variation of pressure coefficient across elevator-nose
seal with angle of attack of the 35° swept-back tail.
Aspect ratio, 4.5; R, 3.0 x 10⁶.

Pressure coefficient across elevator–nose seal, $\frac{\Delta p}{q}$

$\delta_e = -9°$

$\delta_e = -15°$

$A = 4.5$

$\delta_e = -20°$

91 % b
74
45
21

NACA

Angle of attack, a, deg
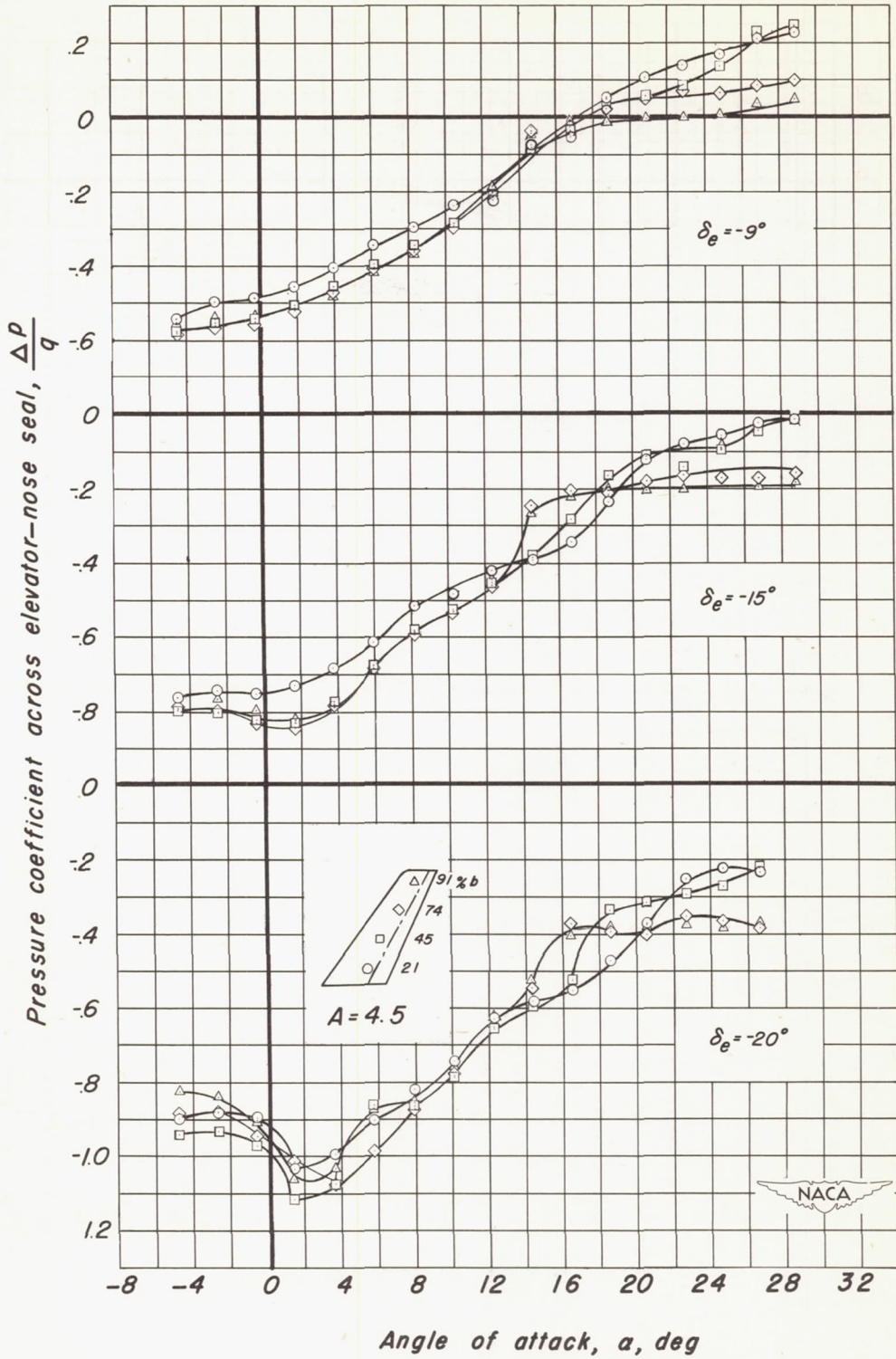
(b) $\delta_e = -9,° -15,° -20.°$

Figure. 11 —concluded.
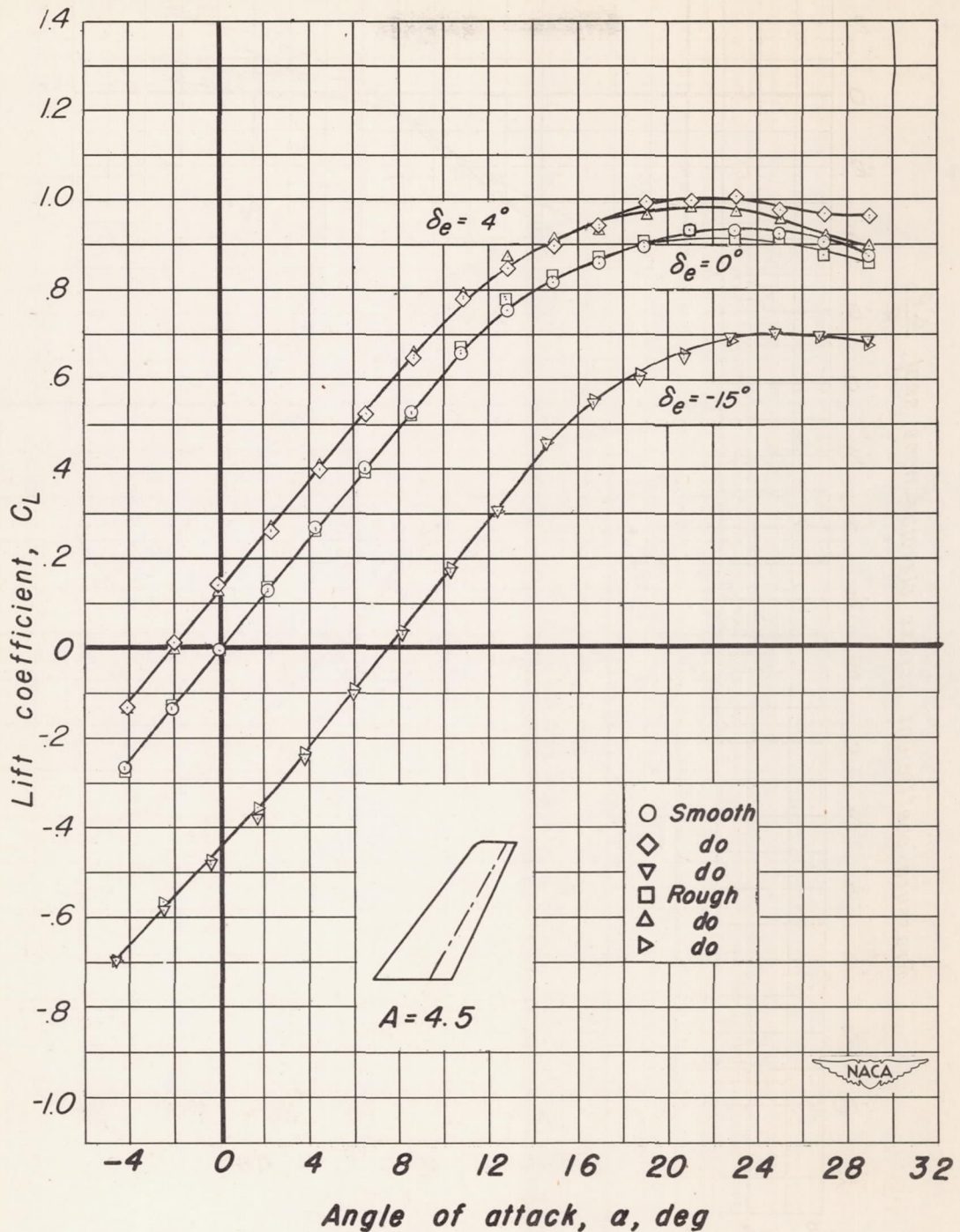
(a) Lift coefficient

Figure 12.— Comparison of the lift and hinge-moment coef-
ficients of the smooth and rough 35° swept-back tail.
Aspect ratio, 4.5; R, 3.0 x 10⁶.
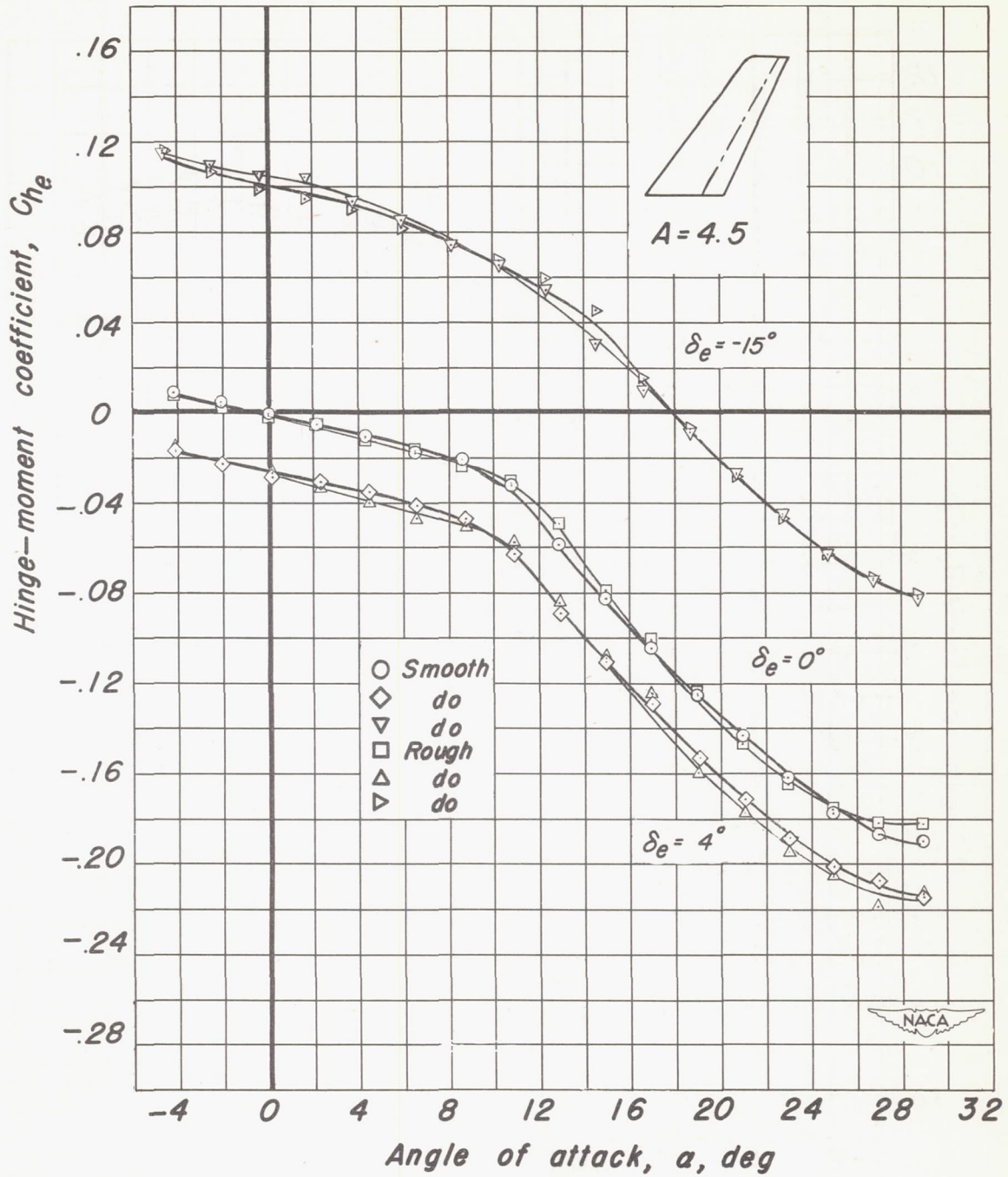
(b) Hinge-moment coefficient

Figure. 12   —concluded.
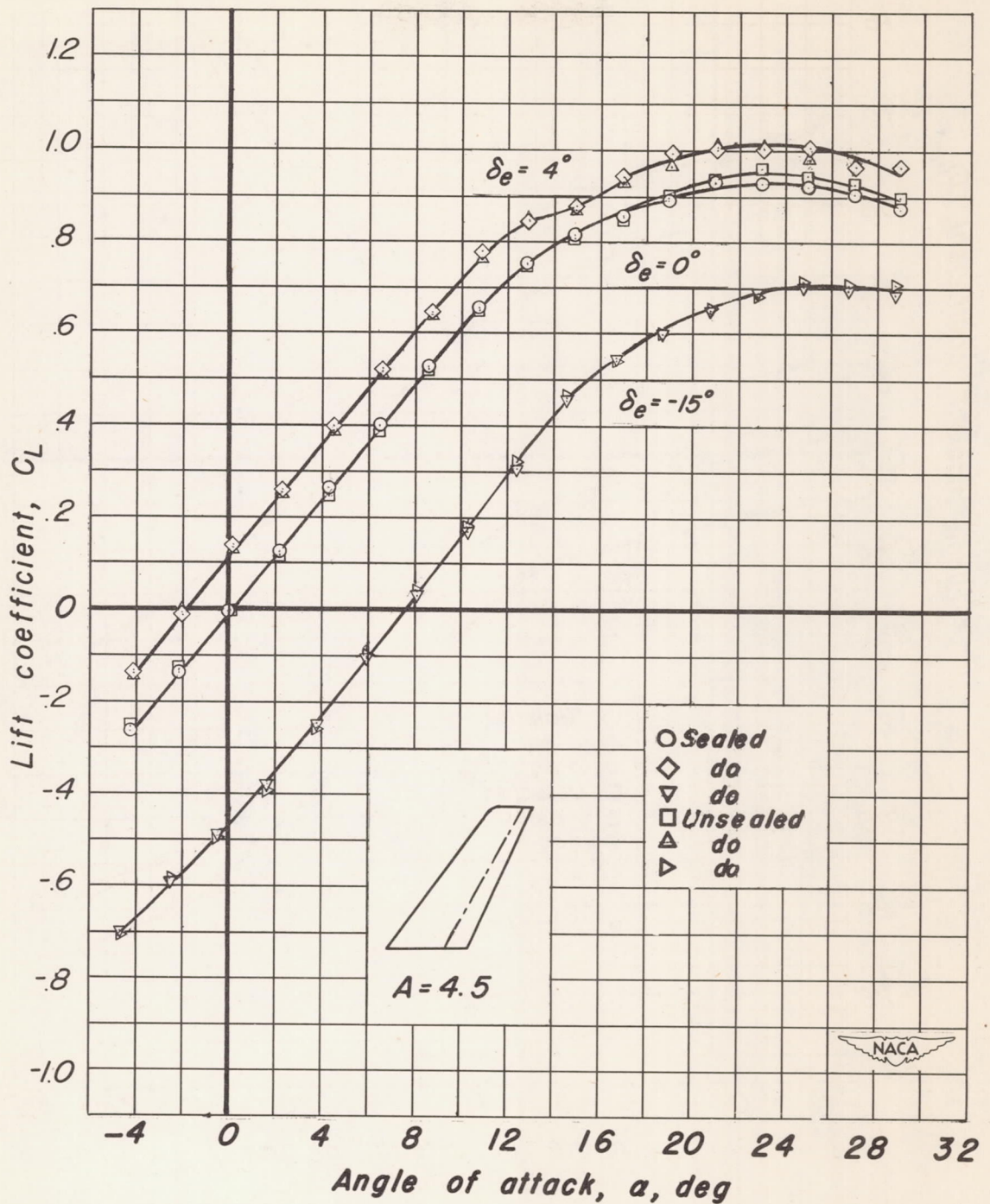
(a) Lift coefficient

Figure 13.— Comparison of the lift and hinge-moment coefficients with and without elevator seal on the 35° swept-back tail. Aspect ratio, 4.5; R, 3.0 x 10^6.
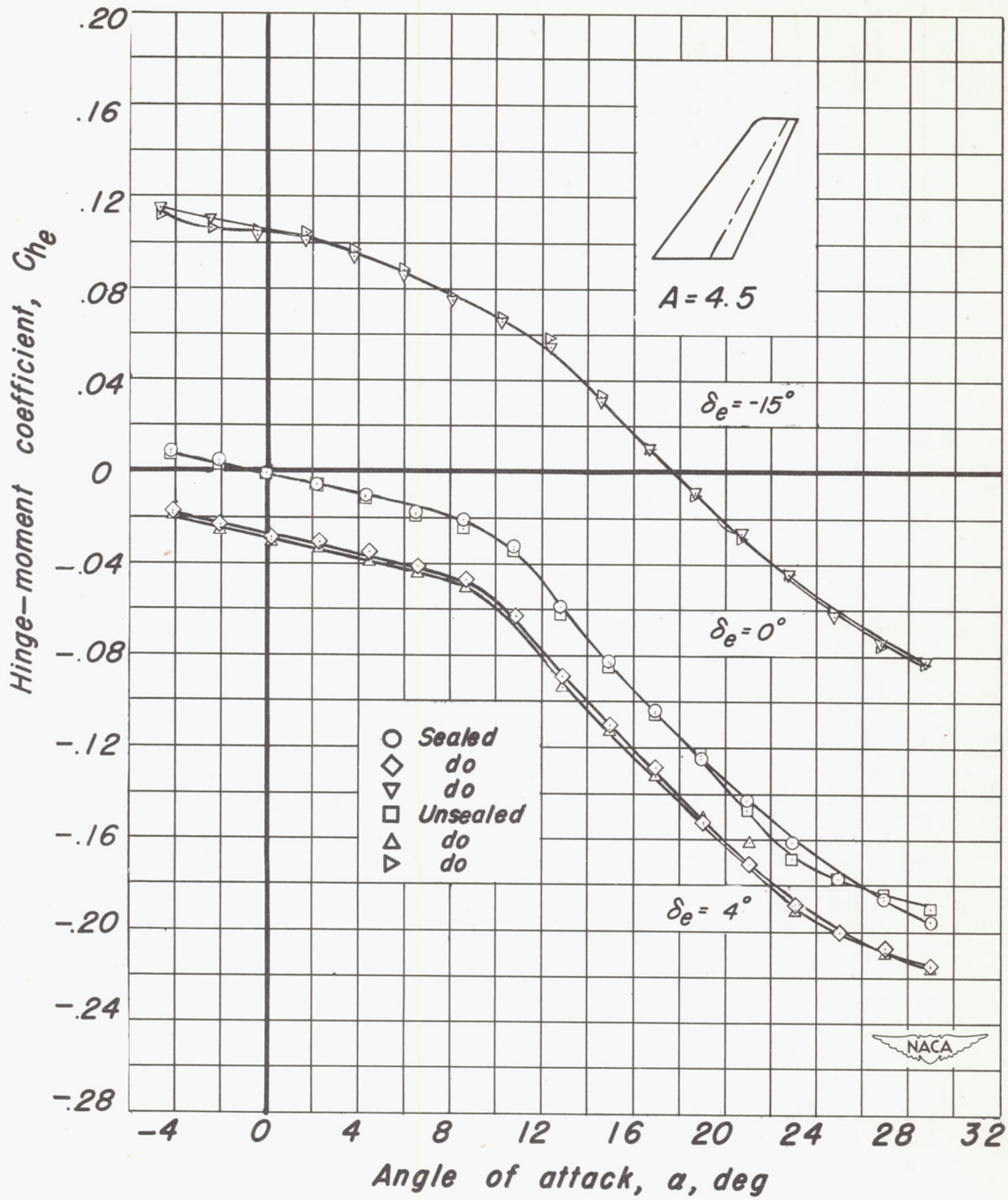
(b) Hinge-moment coefficient

Figure. 13 —concluded.